Harmonic heat flow in anisotropic thin films

Henrik Grönbeck[a] and Michael Reichling[b]
Fachbereich Physik, Freie Universität Berlin, 14195 Berlin, Germany

(Received 17 March 1995; accepted for publication 9 August 1995)

The three-dimensional equation of heat conduction is solved to obtain the time-dependent (harmonic) temperature field in an opaque, thermally anisotropic layer on a thermally thick and isotropic substrate when the system is heated by a modulated Gaussian laser beam. The influence of the anisotropy on the amplitude and phase response of the temperature variation as a function of the position on the surface and depth in the layer is studied. The limiting case of one-dimensional heat diffusion in highly anisotropic media is discussed. For one example the influence of thermal anisotropy on the frequency dependence of the surface temperature distribution is studied. © *1995 American Institute of Physics.*

INTRODUCTION

Thin-film systems have gained a widespread interest in many fields of science and engineering due to their unique physical properties and applicability in many technological areas. The development of manufacturing and preparation techniques has been followed by numerous investigations on the characterization of thin film systems with respect to many physical properties, e.g., morphology, structural, optical, magnetic, and thermal parameters. There is a strong demand for thermal data of thin systems, especially for optical thin films[1–5] and in the rapidly growing field of diamond thin films.[6–13] One of the most striking features of many thin films is their intrinsic anisotropy caused by several mechanisms during film growth.[14–16] The crystalline structure of the films leads to directional effects that introduce an anisotropic behavior for many physical parameters including the thermal conductivity.[17] Anisotropic thermal conduction has been measured for various classes of materials including single crystals,[18,19] composite materials,[20] liquid crystals,[21,22] and superconducting materials[23–25] by various techniques and also plays a role for nondestructive testing.[26] Among various methods applied to this problem, photothermal methods are most feasible in many cases where a noncontact technique is required. The model calculations presented in the present article are devoted to the problem of thermal anisotropy in thin films and its influence on the signal generation in photothermal experiments. They are an extension of recently presented calculations[27] of harmonic heat flow in isotropic layered structures. Here, the three-dimensional equation of heat conduction is solved for a system with an anisotropic layer on a thermally thick substrate heated by a Gaussian laser beam with sinusoidal intensity modulation. Light absorption is restricted to the layer. Extending previously reported results based on a transfer function formalism,[28] we present analytical solutions for the temperature distribution in the layer, the substrate, and the adjacent atmosphere (e.g., air) above the surface of the film. The final expressions for the modulated temperature rise are represented by a two-dimensional Fourier integral that is evaluated with standard numerical routines. Numerical results indicate a strong influence of the nonisotropic diffusion on the temperature distribution. The calculations also provide a possibility to check the validity of one-dimensional models for the flow of heat often used for the interpretation of photothermal measurements.

ANALYTICAL MODEL

The most straightforward way taking the thermal anisotropy of a material into account is to write the Cartesian components of the flux vector $\mathbf{q}$ as a linear function of the temperature gradient[29] at a given point,

$$q_i = -\left(\kappa_{i1}\frac{\partial T}{\partial x_1} + \kappa_{i2}\frac{\partial T}{\partial x_2} + \kappa_{i3}\frac{\partial T}{\partial x_3}\right). \tag{1}$$

The tensor nature of the conductivity (tensor elements κ_{ij}) leads to the important fact that the flow of heat is not necessarily perpendicular to the isothermals as it is in the case of isotropic media. If the anisotropic form of Fourier's law for heat flow is inserted into the equation describing the law of energy conservation we obtain the equation of heat conduction in anisotropic media,

$$\kappa_{11}\frac{\partial^2 T}{\partial x_1^2} + \kappa_{22}\frac{\partial^2 T}{\partial x_2^2} + \kappa_{33}\frac{\partial^2 T}{\partial x_3^2} + (\kappa_{12}+\kappa_{21})\frac{\partial^2 T}{\partial x_1\,\partial x_2} + (\kappa_{13}+\kappa_{31})\frac{\partial^2 T}{\partial x_1\,\partial x_3} + (\kappa_{23}+\kappa_{32})\frac{\partial^2 T}{\partial x_2\,\partial x_3} - \rho c\frac{\partial T}{\partial t} = -Q. \tag{2}$$

Here c and ρ denote the specific heat and mass density, respectively. Q is the source term, i.e., the energy deposited per unit volume and unit time at a given point in the sample. Note that this anisotropic form of the heat conduction equation does not allow a simple separation between diffusivity and conductivity and, hence, these quantities cannot be defined and measured independently as in the case of isotropic heat flow. The model system we consider is schematically shown in Fig. 1. It consists of a thermally anisotropic layer (region 1) with conductivity components κ'_{ij}, an optical absorption coefficient α, and reflectivity R on an isotropic bulk substrate (region 2). Multiple reflections of the laser

[a]Permanent address: Department of Physics, University of Gothenburg and Chalmers University of Technology, 41296 Göteborg, Sweden.
[b]Author to whom correspondence should be addressed; Electronic mail: reichling@matth1.physik.fu-berlin.de

 0021-8979/95/78(11)/6408/6/$6.00

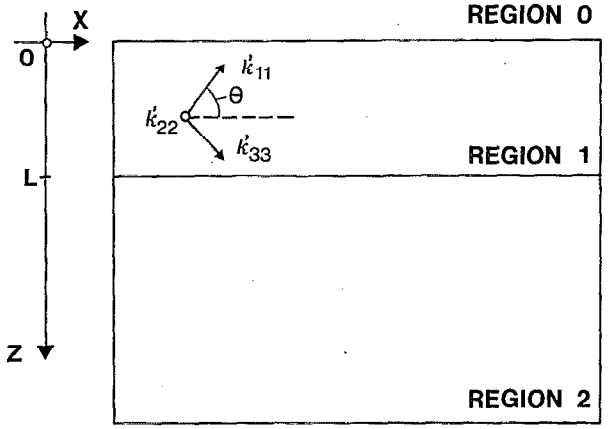

FIG. 1. Model system for an anisotropic layer (region 1) on a thermally thick substrate (region 2). Region 0 is the medium (e.g., air) above the sample. (x,y,z) defines the coordinate system. The y axis is directed perpendicular to the paper plane. κ'_{ij} are the conductivity components of the thin-film sample oriented with an angle θ to the (x,y,z) system.

beam at the interface are neglected. This is a proper presentation of the source term for an opaque film. Semitransparent films would generally require a more complicated description of the internally reflected beams which is not appropriate for an analytical solution. However, the results presented here can also be used as a good approximation for a semitransparent film on a transparent substrate if the reflexion at the interface is weak. The system is irradiated with a Gaussian laser beam (beam radius a and power P) and harmonically modulated with the frequency ω. Light absorption in region 1 yields for the source term

$$Q=2(1-R)\frac{\alpha P}{\pi a^2}e^{-2[(x^2+y^2)/a^2]}e^{-\alpha z}e^{i\omega t}. \tag{3}$$

Since we are only interested in harmonic heat flow the constant term in the source term and consequently the slow rise in average temperature before equilibrium is reached is neglected. Following the model introduced by Iravani and Nikoonahad[28] the anisotropy is restricted to different conductivities in two directions, i.e., we assume a diagonal conductivity κ'_{ij} with two elements equal, yielding the same conductivity in all directions of one plane and a different conductivity perpendicular to this plane,

$$\begin{pmatrix} \kappa'_{11} & 0 & 0 \\ 0 & \kappa'_{11} & 0 \\ 0 & 0 & \kappa'_{33} \end{pmatrix}. \tag{4}$$

The orientation of the principal axis of the conductivity with respect to the sample coordinates (x,y,z) is defined by introducing the polar angle θ between the y axis and the κ'_{33} direction. The conductivity elements in the sample coordinate system (see Fig. 1) are found by a simple tensor transformation of the matrix elements in Eq. (4),

$$\begin{aligned}
\kappa_{11}&=\kappa'_{11}\cos^2\theta+\kappa'_{33}\sin^2\theta,\\
\kappa_{13}&=\kappa_{31}=(\kappa'_{33}-\kappa'_{11})\cos\theta\sin\theta,\\
\kappa_{33}&=\kappa'_{33}\cos^2\theta+\kappa'_{11}\sin^2\theta,\\
\kappa_{22}&=\kappa'_{22}=\kappa'_{11}.
\end{aligned} \tag{5}$$

Assuming that heat transfer is restricted to conduction, the solutions for the temperature are governed by three differential equations, one for each region denoted by the respective subscript,

$$\begin{aligned}
&\kappa_0\nabla^2T_0-\rho_0c_0\frac{\partial T_0}{\partial t}=0,\\
&\kappa_{11}\frac{\partial^2T_1}{\partial x^2}+\kappa_{22}\frac{\partial^2T_1}{\partial y^2}+\kappa_{33}\frac{\partial^2T_1}{\partial z^2}+2\kappa_{13}\frac{\partial^2T_1}{\partial x\,\partial z}\\
&\quad-\rho_1c_1\frac{\partial T_1}{\partial t}=-Q,\\
&\kappa_2\nabla^2T_2-\rho_2c_2\frac{\partial T_2}{\partial t}=0.
\end{aligned} \tag{6}$$

Here κ_0, ρ_0, c_0 and κ_2, ρ_2, c_2 denote conductivity, density, and specific heat of the adjacent atmosphere and the backing substrate, respectively, while κ_{ij}, ρ_1, and c_1 characterize the thin film. The method applied for solving Eqs. (6) follows the one proposed by Iravani and Nikoanahad[28] using a two-dimensional Fourier transform defined as

$$F(u,v)=\frac{1}{2\pi}\int_{-\infty}^{\infty}dx\int_{-\infty}^{\infty}dy\,f(x,y)e^{i(ux+vy)}, \tag{7}$$

where u and v are transformation coordinates. Applying the Fournier transforms to Eqs. (6), we obtain for the temperatures in the three regions

$$\begin{aligned}
T_0(x,y,z,t)&=\frac{1}{2\pi}\int_{-\infty}^{\infty}\int_{-\infty}^{\infty}d\xi\,d\eta\,C(\xi,\eta)\\
&\quad\times e^{\gamma_0 z}e^{-i(\xi x+\eta y)}e^{i\omega t}+\text{c.c.},\\
T_1(x,y,z,t)&=\frac{1}{2\pi}\int_{-\infty}^{\infty}\int_{-\infty}^{\infty}d\xi\,d\eta[\Gamma(\xi,\eta)e^{-\alpha z}\\
&\quad+A(\xi,\eta)e^{\gamma_{11}z}+B(\xi,\eta)e^{\gamma_{12}z}]\\
&\quad\times e^{-i(\xi x+\eta y)}e^{i\omega t}+\text{c.c.},\\
T_2(x,y,z,t)&=\frac{1}{2\pi}\int_{-\infty}^{\infty}\int_{-\infty}^{\infty}d\xi\,d\eta D(\xi,\eta)\\
&\quad\times e^{-\gamma_2(z-l)}e^{-i(\xi x+\eta y)}e^{i\omega t}+\text{c.c.},
\end{aligned} \tag{8}$$

where c.c. denotes the complex conjugate of the respective double integrals and

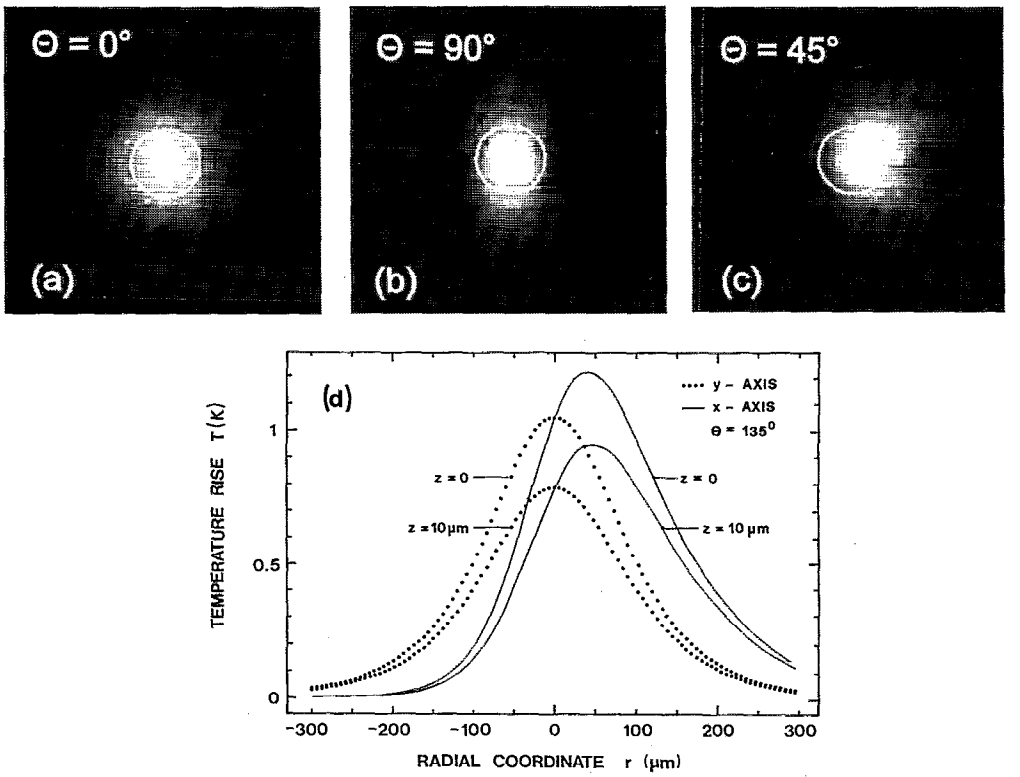

FIG. 2. (a)–(c) Temperature pattern (500×500 μm^2) on the surface of an anisotropic bulk material as a function of the direction θ of the anisotropy. Parameters: $\kappa'_{11}=\kappa_{22}=250$ W/mK, $\kappa'_{33}=80$ W/mK, $\rho=2.25\times10^3$ kg/m^3, $c=714$ J/kg K, $\omega/2\pi=500$ Hz. Circles denote the $1/e^2$ level of the Gaussian heating laser beam. (d) Depth dependence of radial temperature distribution for $\theta=135°$.

$$\Gamma=(1-R)\,\frac{\alpha P}{2\pi}\,e^{[-a^2(\xi^2+\eta^2)]/8}\,\frac{1}{(\nu\alpha-\alpha^2\lambda-\mu)},$$

$$\gamma_{11}=\frac{1}{2\lambda}\,(-\nu+\sqrt{\nu^2-4\lambda\mu}),\quad \gamma_{12}=\frac{1}{2\lambda}(-\nu-\sqrt{\nu^2-4\lambda\mu}),$$

$$\gamma_0=\sqrt{\xi^2+\eta^2+i(\rho_0c_0\omega/\kappa_0)},\qquad (9)$$

$$\gamma_2=\sqrt{\xi^2+\eta^2+i(\rho_2c_2\omega/\kappa_2)},$$

$$\lambda=\kappa_{33},\quad \nu=-2i\xi\kappa_{13},\quad \mu=-(\kappa_{11}\xi^2+\kappa_{22}\eta^2+i\omega\rho_1c_1).$$

The three terms in the expression for the temperature in region 1 represent the temperature rise due to direct heating, a thermal wave generated at the surface propagating into the material, and a wave reflected at the film/substrate interface. Since the substrate is assumed to be thermally thick, a reflected wave does not occur in the solution for region 2. The coefficients A, B, C, and D are determined by applying the boundary conditions at the interface, i.e., continuity in heat flux and temperature to the expression from Eq. (8),

$$T_0=T_1,\quad \kappa_0\frac{\partial T_0}{\partial z}=\kappa_{31}\frac{\partial T_1}{\partial x}+\kappa_{33}\frac{\partial T_1}{\partial z}\quad \text{for } z=0,$$

$$T_1=T_2,\quad \kappa_{31}\frac{\partial T_1}{\partial x}+\kappa_{33}\frac{\partial T_1}{\partial z}=\kappa_2\frac{\partial T_2}{\partial z}\quad \text{for } z=1. \qquad (10)$$

We obtain

$$A=-\frac{\left(\frac{\kappa_2\gamma_2+r}{\kappa_2\gamma_2+\upsilon}\right)e^{-\alpha l-\gamma_{12}l}+\left(\frac{r-\kappa_0\gamma_0}{\kappa_0\gamma_0-\upsilon}\right)}{\left(\frac{s-\kappa_0\gamma_0}{\kappa_0\gamma_0-\upsilon}\right)+\left(\frac{\kappa_2\gamma_2+s}{\kappa_2\gamma_2+\upsilon}\right)e^{\gamma_{11}l-\gamma_{12}l}}\,\Gamma,$$

$$B=\frac{r-\kappa_0\gamma_0}{\kappa_0\gamma_0-\upsilon}\,\Gamma+\frac{s-\kappa_0\gamma_0}{\kappa_0\gamma_0-\upsilon}\,A, \qquad (11)$$

$$C=A+B+\Gamma,\quad D=\Gamma e^{-\alpha l}+Ae^{\gamma_{11}l}+Be^{\gamma_{12}l},$$

where r, s, and υ denote

$$r=-\tfrac{1}{2}\nu-\alpha\lambda,\quad s=-\tfrac{1}{2}\nu-\gamma_{11}\lambda,\quad \upsilon=-\tfrac{1}{2}\nu+\gamma_{12}\lambda.$$

Note that this result may be reduced to the solution for the isotropic case if we assume equal values for all elements of the conductivity tensor for the film. Applying the integral representation for the Bessel function[30] the expressions derived here reduce to those presented by Jackson *et al.*[31] for an isotropic system.

NUMERICAL RESULTS

The complex double integrals derived in the previous section are evaluated numerically yielding amplitude and phase values for the harmonic temperature variation. To demonstrate the effects of anisotropic heat flow we present two-dimensional plots of the amplitude as a function of either x,y surface coordinates revealing anisotropy in planes parallel to the surface or x,z bulk coordinates revealing an-

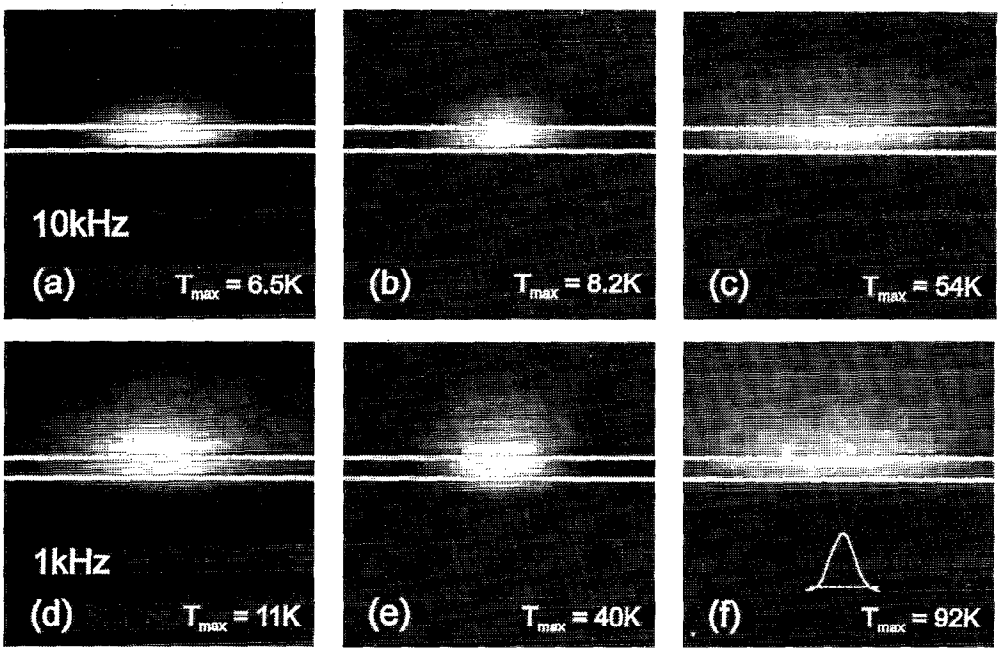

FIG. 3. Temperature distribution in the x/z plane for a 25-μm-thick layer with gold parameters on a glass substrate for two modulation frequencies. Pictures represent: (a), (d): isotropic case; (b), (e): lateral conductivity reduced (1:100); (c), (f): vertical conductivity reduced (1:100); T_{max}: temperature rise at the center of the heating beam. The inset in (f) shows the Gaussian profile of the heating laser beam where the dashed line denotes the $1/e^2$ level.

isotropy with respect to vertical and lateral heat flow, respectively. Calculations were performed for bulk samples and layer-on-substrate systems including heat loss to the ambient atmosphere (air).

Figure 2 shows a calculation for a bulk model system. In Fig. 2(a) the conductivity in the surface plane is uniform ($\kappa_r = \kappa_{11} = \kappa_{22}$) so that the temperature distribution preserves the radial symmetry of the exciting Gaussian laser beam. The extension of the profile beyond the beam size is roughly determined by the lateral thermal length $L_{th} = \sqrt{2\kappa_r/\rho c\omega}$. An elliptical temperature distribution is found for a plane anisotropy corresponding to the condition $\theta = 90°$ as shown in Fig. 2(b). Here the conductivity along the y direction is three times larger than in the x direction leading to a preferred heat flow in this direction. Of course, this effect is only apparent if the thermal length along the y direction is larger than the radius of the incident laser beam.

If the principal axes of the conductivity tensor are not aligned with the sample coordinate system, a steering effect is achieved [Fig. 2(c)]. Such an example with a net conductivity along the positive x axis larger than in the negative direction yields a maximum of the temperature rise shifted along the positive x axis.[32] From the figures presented here it is obvious that anisotropies yielding different components of the conductivity tensor in planes parallel to the surface may easily be determined by any photothermal technique capable of measuring surface temperature distributions provided the modulation frequency is chosen properly. In Fig. 2(d) we also investigate the shift of the maximum as a function of depth (z coordinate). For better clarity only one-dimensional line scans along the x and y axis are shown for $z = 0$ and $z = 10$ μm. As expected the maximum of the temperature is again shifted in positive x direction when probing the temperature distribution below the surface. Actually, it can be shown that the lateral shift depends linearly on the z coordinate.[33]

As an example for a nonisotropic film-on-substrate structure we modeled a system consisting of a film with the thermal parameters of gold but introduced a lateral conductivity that is 1/100 of the one in the vertical direction (311 W^{-1} mK^{-1}) on a glass substrate. Numerical results for 1 and 10 kHz modulation frequency are shown in Figs. 3(b) and 3(e). For comparison the isotropic counterparts are included in Figs. 3(a) and 3(d). The lateral thermal length in the anisotropic case does not allow for heat diffusion beyond the radius of the incident laser beam yielding an alignment of the isothermals in vertical direction at low frequencies [Fig. 3(e)]. The higher temperature in the center of the incident beam is, therefore, preserved almost throughout the entire film thickness. Since the influence of anisotropy on the temperature profile is determined by the lateral thermal length it can be removed by increasing the modulation frequency [Fig. 3(b)]. It is interesting to recognize that at 10 kHz the peak temperature modulation is only 25% higher than for the isotropic case [Fig. 3(a)] while the ratio of peak temperatures is four at 1 kHz [Figs. 3(d) and 3(e)]. This result strikingly demonstrates the importance of lateral diffusion within the film for the shape of the thermal profile at low modulation frequencies. We also calculated a case where the vertical conductivity is 1/100 of the lateral. Results are shown in Figs. 3(c) and 3(f). The thermal length in lateral direction now equals the one for the isotropic calculation, however, the heat is channeled in the lateral direction just beneath the surface leading to a broader temperature profile. Due to the poor diffusion in vertical direction the maximum surface temperature is by a factor of 8 higher than in the isotropic

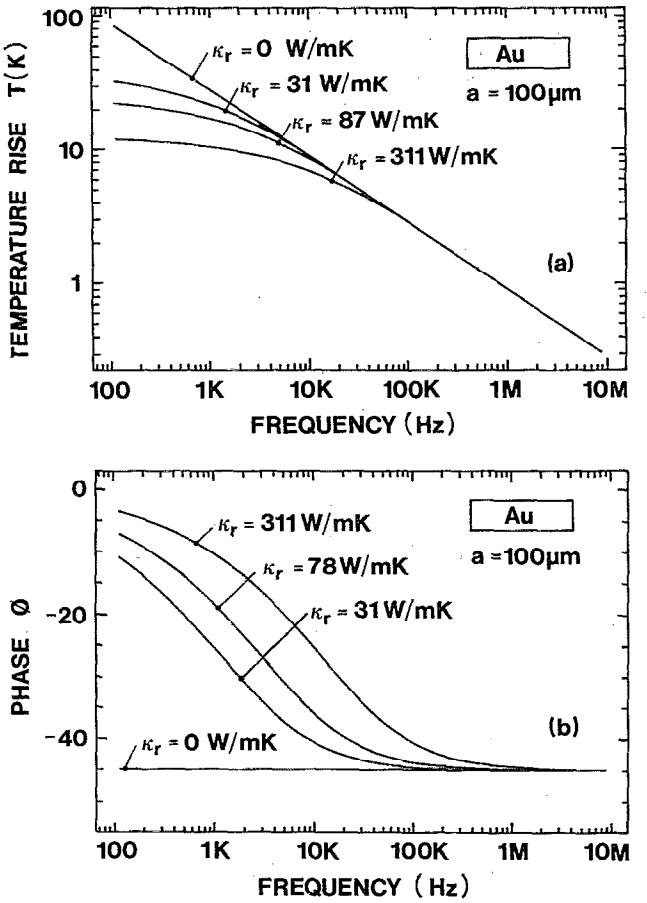

FIG. 4. Frequency-dependent (a) amplitude and (b) phase for a model system using gold thermal parameters varying the conductivity in radial direction. Temperature and phase are calculated at the sample surface in the center of the heating beam.

case. Also note the fact that at low frequencies the heat penetrates far into the ambient atmosphere [Fig. 3(f)].

As pointed out in our previous calculation[27] the frequency dependence of the photothermal response is most helpful for thin-film conductivity measurements. Therefore, we investigated the frequency-dependent amplitude and phase of the surface temperature for different values of the lateral conductivity ranging from 0 to the value of the vertical conductivity. Such studies are a test for the validity of one-dimensional model calculations often used for photothermal wave calculations.[34,35] The basic result for a bulk system with thermal properties of gold is shown in Fig. 4. The curves demonstrate that the saturation of the temperature amplitude observed at low frequencies arises from lateral diffusion and vanishes as the lateral thermal length becomes smaller than the beam radius [Fig. 4(a)]. From Fig. 4(b) it is immediately apparent that the influence of lateral heat flow on the phase extends to much higher frequencies as expected from the amplitude curves. Consequently, even for a large diameter beam radius of 100 μm a one-dimensional model for the heat transport is only justified for frequencies above 1 MHz. For a smaller beam diameter this limit would appear at even higher frequencies. Since such considerations also apply for layered systems we regard this result as a justification for our efforts to calculate an elaborate, rigorous three-dimensional model for the description of photothermal waves in thin-film systems as presented in our previous article.[27] This appears to be especially important when dealing with techniques that are sensitive to the phase of the photothermal signal, and operate with high lateral resolution, such as photothermal microscopy.[36] In such measurements highly focused (~1 μm diameter) laser beams modulated with frequencies in the MHz regime are applied to detect subsurface thermal inhomogeneities and the photothermal phase is used for their localization in depth. From the above mentioned considerations it is evident that a precise depth measurement based on phase measurements strictly requires a three-dimensional thermal model for quantitative image interpretation.

CONCLUSIONS

We presented a complete three-dimensional analytical model describing harmonic heat flow in an absorbing, thermally anisotropic layer on a transparent substrate heated by a Gaussian laser beam. The strong influence of anisotropy on both the maximum temperature amplitude as well as the temperature distribution at the surface and in the depth of the material was demonstrated. Thermal anisotropy in planes parallel to the surface can easily be obtained by photothermal measurements of thermal profiles on the surface at low modulation frequencies. By calculating the frequency dependence of temperature amplitude and phase for systems with different anisotropies we also demonstrated that a three-dimensional model for the heat conduction is absolutely necessary for a valid description of the photothermal phase unless operating at very high frequencies.

ACKNOWLEDGMENTS

The authors are grateful to E. Matthias for continued encouragement and support for this work. This work was supported by the Sonderforschungsbereich 337 of the Deutsche Forschungsgemeinschaft.

[1] D. L. Decker, C. G. Koshigoe, and E. J., Ashly, NBS Spec. **727**, 2911 (1984).
[2] D. Ristau and J. Ebert, Appl. Opt. **25**, 4571 (1986).
[3] S. D. Jacobs, Lab. Laser Energ. Rev. **29**, 30 (1986).
[4] A. H. Guenther and J. K. McIver, Proc. SPIE **895**, 246 (1988).
[5] A. H. Guenther and J. K. McIver, Thin Solid Films **113**, 203 (1988).
[6] O. Käding, E. Matthias, R. Zachi, and H. J. Füsser, Diamond Rel. Mater. **3**, 1178 (1994).
[7] K. Plamann, D. Fournier, E. Auger, and A. Giquel, Diamond Rel. Mater. **3**, 752 (1994).
[8] D. G. Our, A. Witch, Y. Z. Qiu, T. R. Fleischer, L. Wei, P. K. Kuo, R. L. Thomas, and R. W. Pryor, Phys. Rev. B **42**, 1104 (1990).
[9] K. Baba, Y. Aikawa, and N. Shokata, J. Appl. Phys. **69**, 7313 (1991).
[10] T. R. Anthony, J. L. Fleischer, J. R. Olson, and D. G. Cahill, Phys. **69**, 8122 (1991).
[11] G. Lu and W. T. Swann, Appl. Phys. Lett. **59**, 1565 (1991).
[12] K. P. Kuo, L. Wei, R. L. Thomas, and R. W. Pryor, in *Photoacoustic and Photothermal Phenomena III*, Springer Series in Optical Science, Vol. 69, edited by D. Bicanic (Springer, Berlin, 1992), p. 175.
[13] J. E. Gräbner and J. A. Herb, Diamond Films Technol. **1**, 155 (1992).
[14] B. Lewis and J. C. Anderson, *Nucleation and Growth of Thin Films* (Academic, New York, 1978).
[15] H. A. Macleod, J. Vac. Sci. Technol. A **4**, 418 (1986).

[16] J. F. De Natale, A. B. Harker, and J. F. Flintoff, J. Appl. Phys. **69**, 6456 (1991).
[17] L. J. Shaw-Klein, T. K. Hatwar, S. J. Burns, S. D. Jacobs, and J. C. Lambropoulos, J. Mater. Res. **7**, 329 (1992).
[18] A. K. McCurdy, H. J. Maris, and C. Elbaum, Phys. Rev. B **2**, 4077 (1970).
[19] G. Changming and Z. Xiaorong, in *Photoacoustic and Photothermal Phenomena*, Springer Series in Optical Science, Vol. 59, edited by P. Hess and J. Pelzl (Springer, Berlin, 1988), p. 335.
[20] L. J. Inglehart, F. Lepoutre, and F. Charbonnier, J. Appl. Phys. **59**, 234 (1986).
[21] M. Gharbia, A. Hadj-Sahraoui, G. Louis, A. Gharabi and P. Peretti, in *Photoacoustic and Photothermal Phenomena II*, Springer Series in Optical Science, Vol. 62, edited by J. C. Murphy, J. W. MacLachlan-Spicer, L. Aamodt, and B. S. H. Royce (Springer, Berlin, 1990), p. 306.
[22] C. Glorieux, E. Schoubs, and T. Thoen, in *Photoacoustic and Photothermal Phenomena II*, Springer Series in Optical Science, Vol. 62, edited by J. C. Murphy, J. W. MacLachlan-Spicer, L. Aamodt, and B. S. H. Royce (Springer, Heidelberg, 1990), p. 297.
[23] J. T. Fanton, D. B. Mitzi, A. Kapitulnik, B. T. Khuri-Yakub, and G. S. Kino, Appl. Phys. Lett. **55**, 598 (1989).
[24] X. D. Wu, G. S. Kino, J. T. Fanton, and A. Kapitulnik, Rev. Sci. Instrum. **64**, 3321 (1993).
[25] X. D. Wu, J. G. Fanton, G. S. Kino, S. Ryu, D. B. Mitzi, and A. Kapitulnik, Physica C **218**, 417 (1993).
[26] F. Enguehard, A. Déom and D. Balageas, in *Photoacoustic and Photothermal Phenomena III*, Springer Series in Optical Science, Vol. 69, edited by D. Bicanic (Springer, Berlin, 1992), p. 537.
[27] M. Reichling and H. Grönbeck, J. Appl. Phys. **75**, 1914 (1994).
[28] M. V. Iravani and M. Nikoonahad, J. Appl. Phys. **62**, 4065 (1987).
[29] H. Carslaw and J. Jaeger, *Conduction of Heat in Solids* (Oxford University Press, Oxford, 1959).
[30] T. Arfken, *Mathematical Methods for Physicists* (Academic, New York, 1985).
[31] W. Jackson, N. Amer, A. Boccara, and D. Fournier, Appl. Opt. **20**, 1334 (1981).
[32] Note that this calculation differs from a similar result obtained by Iravani and Nikoonahad (Ref. 28) who observed a shift in opposite direction. We believe our result reflects the true physical effect.
[33] H. Grönbeck, technical report, Freie Universität Berlin, Berlin, 1991.
[34] J. Opsal and A. Rosencwaig, J. Appl. Phys. **53**, 4240 (1982).
[35] G. Amato, G. Benedetto, L. Boarino, M. Maringelli, and R. Spagnolo, Appl. Phys. A **56**, 280 (1991).
[36] M. Munidasa and A. Mandelis, in *Principles and Perspectives of Photothermal and Photoacoustic Phenomena*, Progress in Photothermal and Photoacoustic Science and Technology, Vol. 1, edited by A. Mandelis (Elsevier, New York, 1992), p. 300.